

Thermoelectric power of annealed β Ag₂Se alloy thin films: Temperature and size effects—possibility of a new (β 2) phase at low temperatures

V. Damodara Das and D. Karunakaran

Citation: *Journal of Applied Physics* **67**, 878 (1990); doi: 10.1063/1.345747

View online: <http://dx.doi.org/10.1063/1.345747>

View Table of Contents: <http://scitation.aip.org/content/aip/journal/jap/67/2?ver=pdfcov>

Published by the *AIP Publishing*

Articles you may be interested in

[Thermoelectric power in very thin film thermocouples: Quantum size effects](#)

J. Appl. Phys. **100**, 114905 (2006); 10.1063/1.2388046

[New hightemperature superconducting phase spread alloy thin films](#)

Appl. Phys. Lett. **63**, 1276 (1993); 10.1063/1.109756

[Thickness dependence of the phase transition temperature in Ag₂Se thin films](#)

J. Appl. Phys. **68**, 2105 (1990); 10.1063/1.346565

[Thermoelectric power and electrical resistivity of crystalline antimony telluride \(Sb₂Te₃\) thin films: Temperature and size effects](#)

J. Appl. Phys. **65**, 2332 (1989); 10.1063/1.342823

[Size and temperature effects on thermoelectric power of \$\beta\$ tin thin films](#)

J. Appl. Phys. **54**, 977 (1983); 10.1063/1.332023



Thermoelectric power of annealed β -Ag₂Se alloy thin films: Temperature and size effects—possibility of a new (β_2) phase at low temperatures

V. Damodara Das and D. Karunakaran

Thin Film Laboratory, Department of Physics, Indian Institute of Technology, Madras 600 036, India

(Received 5 June 1989; accepted for publication 28 September 1989)

Thermoelectric power of annealed β -Ag₂Se thin films of different thicknesses has been measured both while heating and cooling by the integral method. It is found that it remains practically constant (in β -Ag₂Se phase) during heating while it is a function of temperature while cooling. The thermoelectric power in both heating and cooling cycles is a function of inverse thickness of the films. The difference in behavior between Ag₂Se films during heating and cooling is attributed to the possible transformation to monoclinic phase during cooling from the original orthorhombic phase during heating. The inverse thickness dependence has been explained by the size effect theories. Important material parameters like carrier concentration, Fermi energy, effective mass of carriers, and energy dependence of the mean free path have been evaluated for the β -Ag₂Se (orthorhombic) phase.

I. INTRODUCTION

Silver selenide undergoes a first-order reversible phase transition around 409 K from a semiconducting orthorhombic/monoclinic structure to a metallic, cubic (bcc) structure.¹⁻³ A considerable amount of work has been done in the past few years on electrical, optical, and structural properties of β -Ag₂Se, the semiconducting low-temperature polymorph of silver selenide.⁴⁻⁶ Thermoelectric studies have received much less attention, but there have been some thermoelectric studies on bulk samples of silver selenide.⁷⁻¹⁰ However, there is little literature to date on the thermoelectric properties of vacuum-evaporated silver selenide thin films. In the present paper, the temperature and the thickness dependencies of the Seebeck coefficient of the low-temperature semiconducting polymorph of vacuum-evaporated Ag₂Se thin films of thicknesses in the range 500–2000 Å and in the temperature range of about 300–400 K during both heating and cooling are reported and discussed.

II. EXPERIMENT

Ag and Se of 99.999% purity in their stoichiometric proportion (2:1) were melted in an evacuated quartz ampoule, and maintained at a temperature of 1000 °C, which is about 100 °C beyond the melting point of the compound, for about 12 hours. It was cooled and annealed at 650 °C for several hours and then cooled further slowly to room temperature. The formation of the compound (low-temperature orthorhombic phase) was confirmed by taking x-ray powder diffraction patterns of the sample from different regions of the ingot.

Ag₂Se alloy thin films of thicknesses between 450–2200 Å were prepared by evaporation of the bulk Ag₂Se alloy from a molybdenum boat on to chemically cleaned glass substrates held at room temperature in a vacuum of 5×10^{-5} Torr. The thickness was measured *in situ* using a quartz crystal thickness monitor, and the deposition conditions were maintained almost the same for all the films.

The x-ray diffractograms of as-grown Ag₂Se films did not exhibit any peaks implying that the films formed were

amorphous. Further, electrical measurements could not be carried out on as-grown Ag₂Se films because of the instability of measurements. Hence, all the Ag₂Se as-grown films were vacuum annealed at 373 K for about 3 h, the duration and temperature of annealing being fixed by trial experimentation. The x-ray diffractograms of the annealed (heat-treated) Ag₂Se films confirmed the crystalline compound formation in the thin-film state (Fig. 1). The diffractogram contains only the peaks corresponding to (020), (040) reflections, of the orthorhombic low-temperature phase, indicating that the films have a fibrous texture with (010) planes of the crystallites parallel to the film plane. Even though no electron microscopic examinations were made, it can be said that the grain size in the Ag₂Se films was of the order of 1500 Å as in the case of Ag₂Te thin films¹¹⁻¹² which were also prepared under similar deposition rates and substrate temperatures in the same vacuum system.

The vacuum during film formation, annealing, and the conductivity measurement was about 5×10^{-5} Torr. The measurement setup, and the method of thermoelectric power measurement have already been explained in an earlier paper.¹³

Briefly, the thermal emf of the films was measured with respect to copper, and the relative thermoelectric power and hence the absolute thermoelectric power of Ag₂Se were derived from these data. The thermoelectric power of copper is $+1.7 \mu\text{V/K}$ and hence about 30 times smaller than Ag₂Se thin films. However, it was taken into consideration in the calculation.

The thermal emf data were least square fitted in a computer using localized spline functions. The computer evaluated the thermoelectric power (slope of the emf versus temperature difference curves) values at different temperatures using the least-square-fitted emf values. These thermoelectric power values were plotted as a function of temperature and thickness normally.

III. RESULTS

Figure 2 shows the plots of thermal emf as a function of temperature difference between the hot and cold ends during

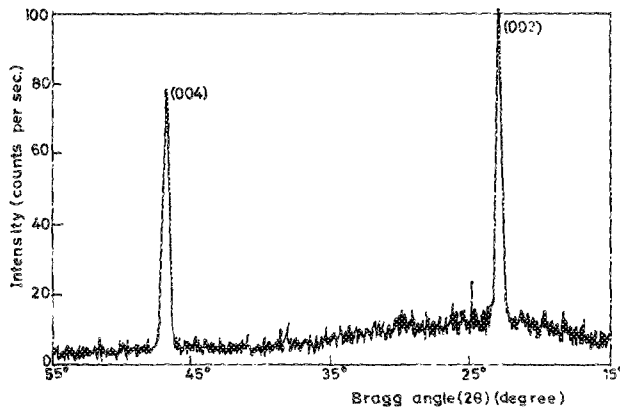


FIG. 1. X-ray diffractogram of a typical annealed Ag_2Se film.

both heating and cooling for an Ag_2Se film of thickness 1130 Å in the temperature range 300–430 K. It is seen from the figure that the heating curve does not coincide with the cooling curve even in the low-temperature semiconducting phase, unlike in the case of Ag_2Te .¹³ Also, during heating, the thermal emf increases linearly with an increase in temperature difference up to a certain point (transformation temperature of about 405 K) and then it increases more slowly at and around the transition point. In the cooling cycle the thermal emf is found to vary nonlinearly with increase of temperature up to the phase transition point. To analyze the dependence of thermoelectric power on temperature, both in the semiconducting phase and at, around, and above the phase transition temperature both during heating and cooling, the thermoelectric power S_F of the

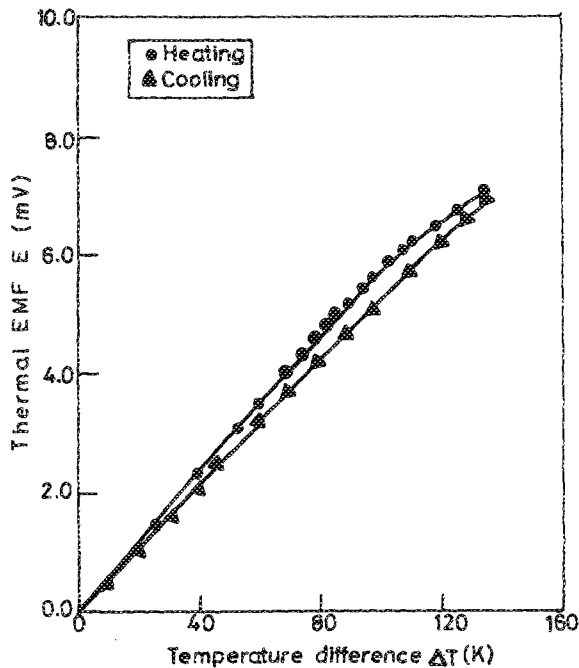


FIG. 2. Thermo emf against temperature difference plot during heating and cooling of Ag_2Se film of thickness 1130 Å.

above film was calculated at different temperatures, and Fig. 3 shows the plot of S_F against temperature. It can be seen from this figure that during heating, the thermoelectric power remains constant with temperature up to the transition point, then falls sharply at the transition point and then rises. During cooling, the thermoelectric power is found to increase linearly with a decrease of temperature below the transition point. Undoped stoichiometric $\beta\text{-Ag}_2\text{Se}$ has been reported to be intrinsic and n type at room temperature. It has also been found impossible to dope Ag_2Se to p type even for materials containing 0.37 at. % excess Se.⁴ In the present observations, the sign of the thermal emf indicates that in Ag_2Se thin films electrons are the predominant carriers.

Figures 4(a) and 4(b) show the plots of thermal emf versus temperature difference for Ag_2Se films of different thicknesses during heating and cooling, respectively, in the semiconducting region. It is seen that during heating the thermal emf is nearly linear with respect to temperature difference. The thermal emf is found to vary nonlinearly with temperature in the cooling cycle up to the phase transition, and it also increases as the film thickness increases for a given temperature difference. Figures 5(a) and 5(b) show the plots of thermoelectric power S_F versus temperature for the above films of different thicknesses during heating and cooling, respectively. It is seen that the thermoelectric power during heating is independent of temperature for all the films in the temperature range 300–400 K; while during cooling, the thermoelectric power is found to increase linearly with a decrease of temperature for all the films. It is also seen that the thermoelectric power increases as the thickness increases.

To analyze the thickness effects during heating, the thermoelectric power at temperatures 300, 340, and 380 K as

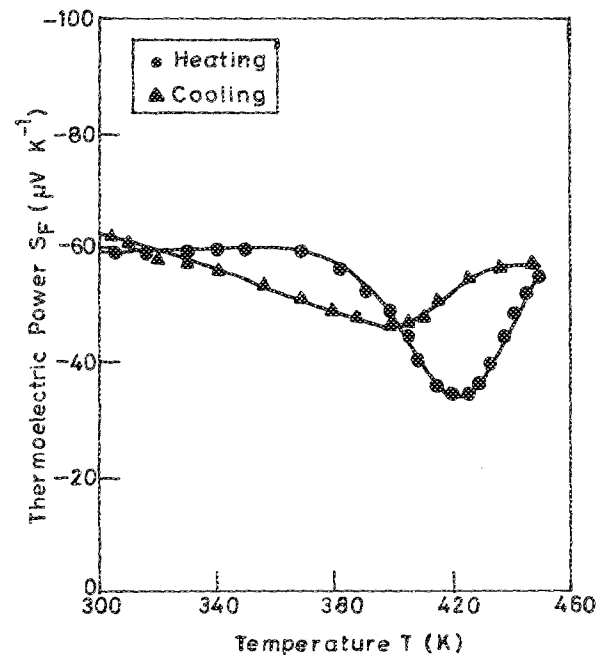


FIG. 3. Thermoelectric power against temperature plot for the film in Fig. 2 during heating and cooling.

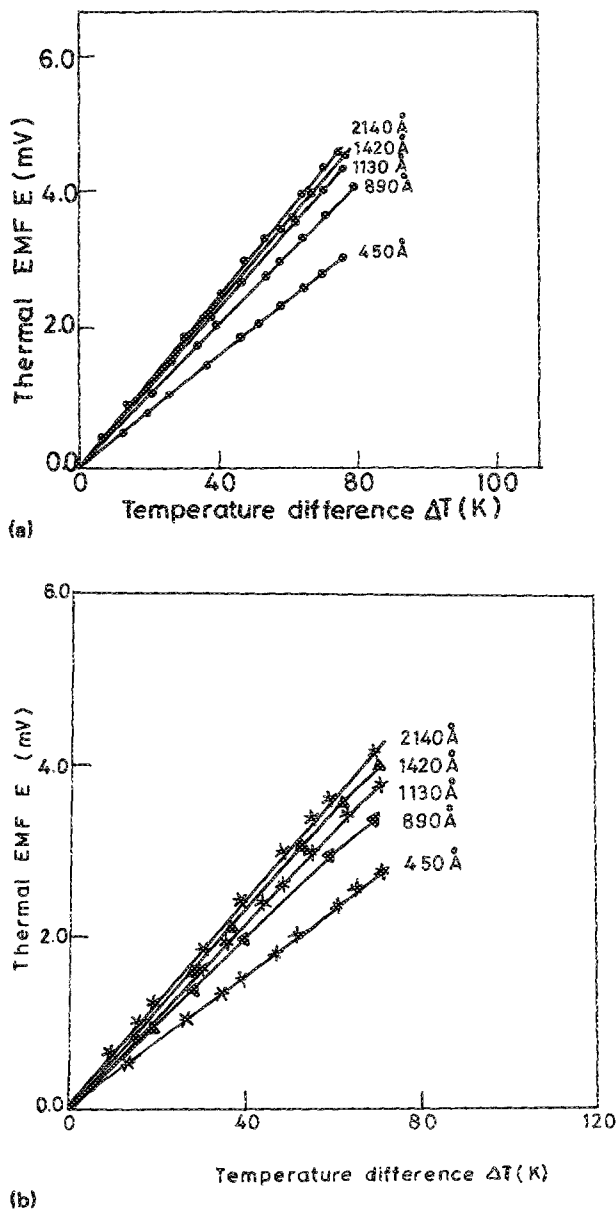


FIG. 4. Thermal emf against the temperature difference plots for different films during (a) heating and (b) cooling.

observed during heating was plotted as a function of reciprocal film thickness. Figure 6 shows it to be linear. It is to be noted that the points corresponding to different temperatures lie on the same straight line.

Similar plots for thermoelectric power during cooling are shown in Fig. 7. It is seen that unlike during heating, the points at different temperatures form different straight lines because the thermoelectric power is temperature dependent. Further, all three curves are linear, indicating an inverse functional relationship between S_F and t . However, it may be noted that the slopes of the three lines are slightly different, the slope increasing with the increase in temperature.

Thus it is seen that the thermoelectric power variation with both temperature and thickness during cooling is different from the behavior while heating. As a result, the thickness dependence and the slopes of the S_F versus $1/t$ plots and

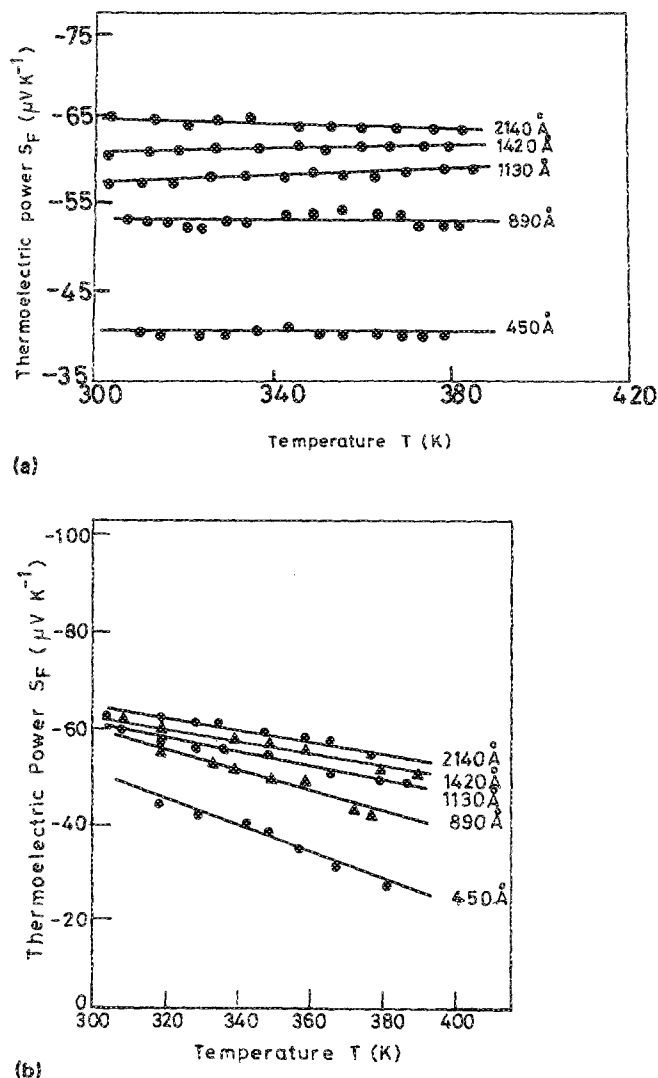


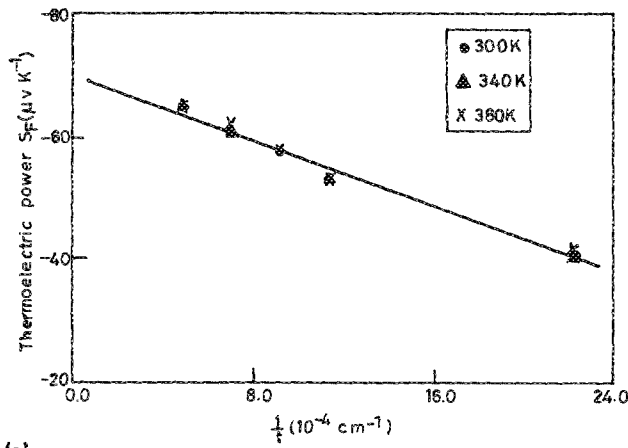
FIG. 5. Thermoelectric power against temperature plots for the films in Fig. 4 during (a) heating and (b) cooling.

also the intercepts will be different for the three temperatures during cooling (unlike during heating), because S_g (the "grain-boundary thermoelectric power", which is the thermoelectric power of the bulk with the thin-film microstructure) will also be a function of temperature. This difference in the behavior of the thermoelectric power during heating and cooling indicates the possibility that the low-temperature phase during cooling is different from that of the original low-temperature phase.

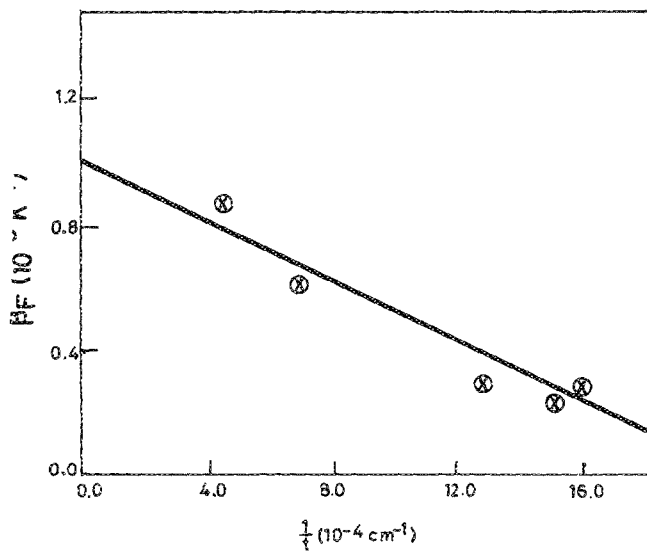
IV. DISCUSSION

A. Temperature dependence

Silver selenide is a narrow band-gap ($E_g = 0.07$ eV/0.18 eV)⁵ semiconducting material with orthorhombic/monoclinic symmetry at room temperature. It is characterized by a high carrier density of the order of 10^{18} cm⁻³ irrespective of the preparation method.¹⁴ Conn *et al.*⁸ report the carrier concentration of bulk Ag₂Se at 300 K as 2.8×10^{18} cm⁻³. In spite of the small value of the band gap, the effective mass of electrons m^* is higher than that of Ag₂Te, i.e.,



(a)



(b)

FIG. 6. (a) Reciprocal thickness dependence of thermoelectric power of Ag_2Se films at three different temperatures (300, 350, and 400 K) during heating. (b) Reciprocal thickness dependence of temperature coefficient of resistance (β_r) at 300 K.

$0.12 m_p$.¹³ Hence, the degeneracy is partial, even through the carrier concentration is high. Almost all the workers identify stoichiometric $\beta\text{-Ag}_2\text{Se}$ as an intrinsic partially degenerate semiconductor, in this temperature range.

According to Conn *et al.*'s⁸ observation on bulk polycrystalline specimens of Ag_2Se , thermoelectric power shows a linear decrease from 106 to 393 K, followed by a sharp fall at the transition temperature of 406 K, then followed by a slow rise. Astakhov *et al.*'s⁷ studies on polycrystalline Ag_2Se show that in the temperature range 93–373 K, the thermoelectric power varies from -200 to $-150 \mu\text{V}/\text{K}$. Junod⁹ also reports a similar behavior for low-temperature $\beta\text{-Ag}_2\text{Se}$ up to the phase transition temperature. While Conn *et al.*'s⁸ studies indicate a decrease in the Seebeck coefficient of only about $40 \mu\text{V}/\text{K}$ through the transition point, those of Junod⁹ show a decrease of about $80 \mu\text{V}/\text{K}$. Shukla *et al.*'s¹⁰ thermo-

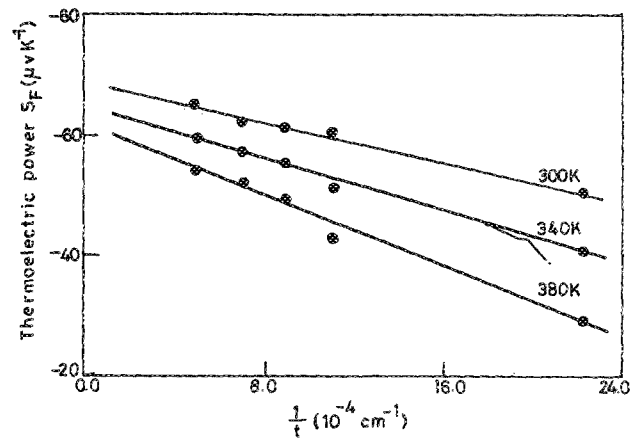


FIG. 7. Reciprocal thickness dependence of thermoelectric power of Ag_2Se films at three different temperatures (300, 350, and 400 K) during cooling.

electric power studies on bulk single-crystal Ag_2Se specimens over a range of composition as a function of temperature show that the Seebeck coefficient is essentially independent of temperature in the low-temperature β phase, while it shows a slight decrease with increase in temperature in the high-temperature α phase. The thermoelectric power does not show any marked change with composition in the β phase. Also the change in thermoelectric power during transition is found to be small.

In the present studies, it is found that thermoelectric power is almost independent of temperature during heating, but in the cooling cycle the thermoelectric power decreases linearly with increase of temperature up to the transition point. Hence, the present studies show that the behavior observed during heating is similar to that of Shukla *et al.*,¹⁰ while the behavior during cooling is similar to that of Conn *et al.*,⁸ Astakhov *et al.*,⁷ and Junod.⁹

The detailed structural studies carried out by electron microscopy techniques on thinned Ag_2Se samples by De Ridder *et al.*² reveal that the low-temperature phase is a pseudo-orthorhombic one, and the high-temperature phase is body-centered cubic. With specific thermal treatment, it is possible to transform the pseudo-orthorhombic into a monoclinic structure.^{2,15–21} During cooling, the bcc selenium lattice, instead of undergoing a transformation to the original pseudo-orthorhombic arrangement, twins on a set of (211) planes and the low-temperature monoclinic phase (e.g., β_2) is obtained by an abrupt ordering of the silver atoms in the twinned selenium bcc lattice. Hence, because of the possibility of formation of pseudophases, the thermoelectric power variation with temperature may exhibit different behavior during heating and cooling. After the second cycle of heating and cooling also, it was found that the new monoclinic phase was found to exist at low temperature (both during heating and cooling) as inferred from the decrease of thermoelectric power with an increase in temperature observed in the films. Apparently the monoclinic phase is a fairly stable metastable phase. This reasoning is strengthened by the fact that earlier workers have made measurements on monoclinic phase (β_2 phase)^{7,8,9} in addition to the orthorhombic (β) phase.¹⁰

B. Thickness dependence

The effective mean-free-path model developed by Pichard *et al.*²² which takes into account the grain-boundary scattering, gives the analytical expression for the Seebeck coefficient of the film as a function of the reciprocal thickness, as

$$S_F = S_g \left(1 - \frac{3}{8} (1-p) \frac{l_g}{t} \frac{U_g}{1+U_g} \right), \quad (1)$$

where S_g is the Seebeck coefficient, l_g the mean free path of the charge carriers, and U_g the energy dependence of the mean free path of carriers in the infinite thick film, and is equal to $U_g = (d \ln l_g / d \ln E) E = E_F$. p is called the specular parameter which gives the fraction of charge carriers incident on the surfaces of the film which is specularly scattered.

It is seen from the above equation that a plot of S_F versus $1/t$ will be a straight line, where the intercept on the y -axis gives S_g . The value of S_g obtained from the slope of the S_F vs $1/T$ heating plot is about $-70 \mu\text{V/K}$ at 300 K (in β phase). The value reported earlier for bulk samples of $\beta\text{-Ag}_2\text{Se}$ is about $-120 \mu\text{V/K}$. The large difference between the thermoelectric power value obtained in thin films and that reported by Conn *et al.*⁸ on bulk polycrystalline samples can be because of the differences in the texture of the material.

1. Estimation of U_g , E_F , and m^*

Considering Eq. (1), and equating the slope

$$\frac{3}{8} (1-p) l_g [U_g (1+U_g)] S_g$$

to 13.46×10^{11} , and treating p as zero (i.e., assuming completely diffuse scattering from the surfaces) and taking l_g and S_g as 1280 \AA (from resistivity data)¹⁶ and $70.11 \mu\text{V/K}$, respectively, the intercept of curve in Fig. 6 (for the β phase), U_g can be evaluated, and it comes about 0.684, so that $l_g \propto E^{0.684}$ at the Fermi energy. The Seebeck coefficient of an infinite thick film is given by²²

$$S_g = (\pi^2 k^2 T / 3eE_F) (1 + U_g). \quad (2)$$

Using this expression (as Ag_2Se is a weakly degenerate semiconductor) and substituting for S_g and U_g and for the other physical parameters, the Fermi energy of electrons is determined to be 0.175 eV. As the Fermi energy and the carrier concentration are known, these values can be used to determine the effective mass of carriers using the expression

$$E_F = (\hbar^2 / 2m^*) (3\pi^2 n)^{2/3}, \quad (3)$$

and the effective mass calculated is about 0.7 times the rest electron mass.

C. Estimation of V and β_0 from thermoelectric and TCR studies

According to Tellier *et al.*,²³ the simultaneous analyses of thermoelectric power data in the form S_F/S_g against the temperature coefficient of resistivity (TCR) ratio β_F/β_g allow the determination of both U and V , the terms representing the energy dependence of bulk mean free path and Fermi surface area. These are given, respectively, by

$$V = \left(\frac{d \ln l_0}{d \ln E} \right)_{E=E_F} \quad \text{and} \quad V = \left(\frac{d \ln A}{d \ln E} \right)_{E=E_F},$$

where l_0 and A are the mean free path and Fermi surface area, respectively. β_F is the TCR of the film and β_g that of a bulk having the thin-film microstructure. The expression given by Tellier *et al.*¹⁶ is

$$\frac{-S_F}{S_g} = -\frac{V}{S_g} S - \left(\frac{U}{S_g} \frac{\beta_g}{\beta_0} S \right) \frac{\beta_F}{\beta_g},$$

where $S = \pi^2 k^2 T / 3eE_F$ and β_0 is the bulk (single-crystal-line) TCR. Hence, the plot of S_F/S_g against β_F/β_g should yield a straight line with an ordinate intercept at $(-V/S_g)S$ and a slope of $-(U/S_g)S(\beta_g/\beta_0)$. From the S_F versus $1/t$ plot [Fig. 6(a)] and the β_F versus $1/t$ plot [Fig. 6(b)], S_F/S_g and β_F/β_g values are generated for different thicknesses at 300 K. Then a plot is drawn as shown in Fig. 8 between S_F/S_g and β_F/β_g . The intercept and the slope come out to be 0.6 and 0.4, respectively.

Equating the intercept, to $-(V/S_g)S$, and substituting for S and S_g , V is determined as 1.003. Hence the energy dependence of Fermi surface area, i.e., $(d \ln A / d \ln E) E = E_F$ is unity and hence the Fermi surface for Ag_2Se turns out to be spherical.

Equating the slope to $-(U/S_g)S(\beta_g/\beta_0)$ and substituting for U , S , S_g and β_g , β_0 the bulk TCR is determined from the studies of $\beta\text{-Ag}_2\text{Se}$ thin films as $1.042 \times 10^{-3} \text{ K}^{-1}$.

V. CONCLUSIONS

It is found from the present study that the thermoelectric power of low-temperature phase Ag_2Se thin films in the thickness range 400–2000 \AA obeys the size effect theories, and that the thermoelectric power is independent of temperature in the temperature range 300–400 K during heating ($\beta\text{-Ag}_2\text{Se}$ phase), and increases linearly with decrease of temperature from the transition point up to 300 K during cooling ($\beta_2\text{-Ag}_2\text{Se}$ phase). The transport parameters such as U_g , E_F , m^* , β_0 , and V have been determined from the studies of $\beta\text{-Ag}_2\text{Se}$ thin films. The evaluated parameters are tabulated in Table I, where a comparison is made with the already published results. The difference in thermoelectric power variation with temperature (and thickness) observed

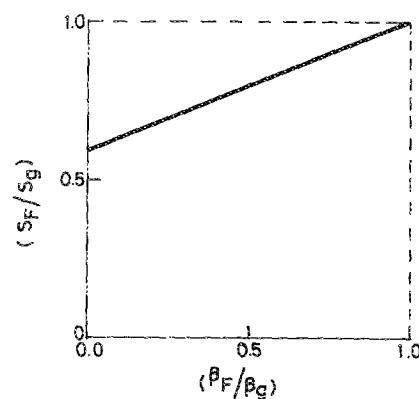


FIG. 8. Plot of S_F/S_g against β_F/β_g for different thicknesses at 300 K.

TABLE I. Comparison of the evaluated electrical parameters for β -Ag₂Se (from thermoelectric studies) with the published results.

Parameter	Present work	Published results (Reference)
Carrier concentration at 300 K	$6.1 \times 10^{18} \text{ cm}^{-3}$	$4.3 \times 10^{18} \text{ cm}^{-3}$ (7) $1 \times 10^{18} \text{ cm}^{-3}$ (3) $2.8 \times 10^{18} \text{ cm}^{-3}$ (24)
Fermi energy (E_F)	0.175 eV	...
Effective mass (m_n^*)	$0.07 m_0$	$0.12 m_0$ (15) $0.17 m_0$ (24)
Bulk TCR (β_0)	$1.04 \times 10^{-3} \text{ K}^{-1}$...
Energy dependence of MFP (U_g)	0.684	...

in the low-temperature range during cooling as compared to that during heating suggests that the phase during cooling (β_2 phase) is different from that during heating (β phase) in the low-temperature region.

¹P. Rahlfs, Z. Phys. Chem. B **31**, 157 (1936).

²R. De Ridder and S. Amelinckx, Phys. Status Solidi A **18**, 99m (1973).

³Y. Baer, G. Busch, C. Frohlich, and E. Steigmehr Z. Naturforsch. **17a**, 886 (1962).

⁴R. Dalven and R. Hill, J. Appl. Phys. **38**, 753 (1967).

⁵R. Dalven and R. Gill, Phys. Rev. **159**, 645 (1967).

⁶Yu. G. Asadov and G. A. Yabraibova, Phys. Status Solidi A **12**, K13 (1972).

⁷O. P. Astakhov and V. D. Golyshev, Inorg. Mater. **10**, 1391 (1974).

⁸J. B. Conn and R. C. Taylor, J. Electrochem. Soc. **107**, 977 (1972).

⁹P. Junod, Helv. Phys. Acta **32**, 567 (1959).

¹⁰A. K. Shukla, H. N. Vasan, and C. N. R. Rao, Proc. R. Soc. London Ser. A **376**, 619 (1981).

¹¹V. Damodara Das and D. Karunakaran, J. Phys. Chem. Solids **46**, 551 (1985).

¹²V. Damodara Das and D. Karunakaran, J. Appl. Physics **66**, 1822 (1989).

¹³V. Damodara Das and D. Karunakaran, Phys. Rev. B **30**, 203 (1984).

¹⁴V. V. Gorbachev and I. M. Putilin, Inorg. Mater. **11**, 1329 (1976).

¹⁵S. A. Aliev, N. A. Verdieva, and M. I. Aliev, Fiz. Tekh. Poluprovodh. **12**, 2075 (1978).

¹⁶V. Damodara Das and D. Karunakaran, Phys. Rev. B **39**, 10872 (1989).

¹⁷N. G. Dhere and A. Goswami, Thin Solid Films **5**, 137 (1970).

¹⁸L. V. Courtantinesur, Thin Solid Films **32**, 333 (1976).

¹⁹Yu. G. Asadov and G. A. Yabraibova, Phys. Status Solidi A **12**, K13 (1972).

²⁰G. A. Ejendiev and I. R. Nuriev, Sov. Phys. Crystallogr. **14**, 787 (1970).

²¹P. Junod, H. Hedizer, B. Kilchor, and J. Wulschleger, Philos. Mag. **36**, 941 (1977).

²²C. R. Pichard, C. R. Tellier, and A. J. Tossier, J. Phys. F **10**, 2009 (1980).

²³C. R. Tellier, A. J. Tossier, and L. Hafid, J. Mater. Sci. **15**, 2875 (1980).

²⁴V. V. Gorbach and I. M. Putilin, Phys. Status Solidi B **69**, K153 (1975).